Revue des Energies Renouvelables Vol. 15 N°4 (2012) 609 – 620

One-step electrodeposited $CuInSe_2$ absorber layers for efficient PV cells

B. Ndiaye, C. Mbow, M.S. Mane and C. Sène*

Laboratoire des Semi-conducteurs et d'Energie Solaire, 'LASES'
Département de Physique, Faculté des Sciences et Techniques
Université Cheikh Anta Diop, Dakar, Sénégal

(reçu le 11 Janvier 2012 – accepté le 28 Décembre 2012)

Abstract - *Thin polycrystalline $CuInSe_2$ (CIS) films for photovoltaic (PV) applications were deposited on molybdenum (Mo)-coated soda lime glass substrates by the one-step electrodeposition process. Films growth was carried out using low concentration aqueous sulfate-based single baths containing dilute $CuSO_4.5H_2O$, $In_2(SO_4)_3.H_2O$ and SeO_2. The electrodeposited CIS layers were studied using SEM, EDS, X-ray diffraction and optical analyses. It was found that film microstructure, composition and morphology strongly depend on the initial concentrations of Cu(II), In(III) and Se(IV) electro-active ionic species in the electrochemical bath. Investigations on the films structure have shown that as-deposited samples are composed of microcrystalline and/or amorphous materials and require recrystallization at high temperature for device processing. Annealing in H2Se atmosphere at 450 °C led to highly crystallized thin films exhibiting the chalcopyrite structure with a pronounced (112) orientation. Optimized processing conditions for high quality thin CIS absorber materials have been established and subsequent photovoltaic (PV) devices exhibited ~ 9% efficiency.*

Résumé - *Des couches minces polycristallines de $CuInSe_2$ (CIS) pour des applications photovoltaïques ont été déposées sur des substrats de verre sodé recouvert d'une fine couche de molybdène (Mo) par la méthode de l'électrodéposition. La croissance des films a été réalisée en utilisant des bains aqueux à base de sulfate, faiblement concentrés contenant $CuSO_4.5H_2O$, $In_2(SO_4)_3H_2O$ and SeO_2. Les couches minces de CIS électrodéposées ont été étudiées en utilisant la microscopie électronique à balayage (MBE), la spectroscopie par dispersion d'énergie (SDE), la diffraction aux rayons X (DRX) et des analyses optiques. Il a été trouvé que la microstructure, la composition atomique et la morphologie des films dépend fortement de la concentration initiale des espèces ioniques électro-actives Cu(II), In(III) et Se(IV) dans le bain électrochimique. L'étude de la structure des films a montré que les films fraîchement déposés sont composés de matériaux microcristallins et/ou amorphes et nécessitent une recristallisation à température élevées pour la réalisation des dispositifs photovoltaïques. Le traitement thermique à 450 °C sous atmosphère de sélénium conduit à des couches minces fortement cristallisées mettant en évidence la structure chalcopyrite avec une forte orientation préférentielle correspondant au plan (112). Les conditions optimales permettant d'élaborer des matériaux absorbeurs en couches minces de CIS de haute qualité ont été établies et les dispositifs photovoltaïques réalisés avec ces couches donnent des rendements de conversion proches de 9 %.*

Keywords: Copper Indium Selenide - Absorber layers – Electrodeposition - Photovoltaic devices.

1. INTRODUCTION

Copper indium diselenide ($CuInSe_2$) and related compounds have shown very promising performances as absorber materials in thin film photovoltaic applications. At

* chksene@yahoo.fr

laboratory scale, solar cells with efficiencies as high as almost 20 % have now been developed [1-3].

To achieve these high efficiencies, PV devices are processed using high vacuum-based technologies, when in fact one of the challenges in photovoltaic research is the use of simple, low cost and large-area processes of high quality material processing. Non-vacuum alternatives growth methods such as chemical bath deposition (CBD), spray pyrolysis, electrodeposition, etc, have been investigated.

Electrodeposition is of the most appealing and is now an important area of research in thin film advanced material processing. It is particularly interesting because it requires low cost equipment and allows deposition of uniform large area films together with high material yield and a good control of the overall film composition and thickness by electrical or chemical parameters.

In thin film photovoltaic applications, it is therefore a potentially suitable route for material processing. Electrodeposition has successfully been used in the fabrication of CdTe thin films for use in PV devices leading to near commercial performance [4] and chalcopyrite layers for use in thin film solar cells [5, 6].

In the case of PV devices using electrodeposited $CuInSe_2$ films as absorber layers, a wide range of efficiencies has been reported. However, the most efficient of these devices always involved a PVD step in the CIS absorber fabrication [6, 7]. Photovoltaic devices with a CIS absorber layers made using only the one-step electrodeposition show low efficiencies [8-10].

In this work, electrodeposition of CIS layers using sulfate-based plating solutions is described. At a given deposition potential, the effect of bath concentrations on the chemical composition and morphology of the electrodeposited CIS films have been investigated. This makes it possible to define best bath concentrations leading to high quality CIS films for PV devices applications.

2. EXPERIMENTAL

CIS samples were single bath electrodeposited using a Princeton Applied Research (PAR) Potentiostat/Galvanostat Model 173 and a vertical three-electrode cell setup. A saturated calomel electrode (SCE) was used as a reference electrode and a Pt gauze as a counter electrode. Films deposition were performed potentiostatically on 2 cm × 2 cm dc-sputtered 0.7 µm Mo-coated soda-lime glass used as working electrode. For optical analyses, CIS samples were grown on transparent conducting ITO substrates.

The plating baths were sulfate-based solutions containing $CuSO_4.5H_2O$, $In_2(SO_4)_3.H_2O$, SeO_2 and $Li_2SO_4.H_2O$ as a supporting salt, dissolved in deionized water. Cu, In and Se were co-deposited from the electrochemical solution at room temperature by a slightly stirring diffusion process. CIS thin films were formed at a constant potential of –0.55 V measured versus saturated calomel electrode for a duration of usually 100 minutes which gave approximately 2 - 2.5 µm thick layers.

The post-deposition treatments of the electrodeposited CIS films were carried out in a flowing 0.35 % H_2Se/Ar (g) (Scott Specialty Gases) atmosphere in a horizontal laminar flow thermal chemical vapor deposition reactor at atmospheric pressure, as described elsewhere [11]. Heat treatment temperature and duration were 450 ºC and 20 minutes respectively. Surface morphology was evaluated by scanning electron microscopy (SEM) in an Amray 1810 T SEM.

The composition of the samples was measured by energy dispersive X-ray spectroscopy (EDS) at 20 kV using a vertically incident beam with an Oxford INCA system in the Amray 1810 T SEM. X-ray diffraction analyses were performed using a Philips/Norelco Bragg-Brentano focusing diffractometer with a CuK_α X-ray tube at 35 kV.

Optical analyses on CIS films coated on transparent ITO substrates were carried out using a Perkin- Elmer Lambda-9 UV-visible-IR Spectrophotometer fitted with integrating sphere.

Photovoltaic devices were completed according to the fabrication method used by Shafarman *et al.* [12], which involves a 50 nm chemically bath deposited CdS buffer layer, sputtered intrinsic ZnO and highly conductive Al-doped ZnO window layers and finally a Ni-Al grid to reduce resistive losses. Current-voltage ($J-V$) characteristics were recorded under AM 1.5 (100 mW/cm^2) sun simulation at 25 °C, using an Oriel Xenon solar simulator.

3. RESULTS

Electrodeposition of $CuInSe_2$ and related compounds is often carried out using Cu(II) and Se(IV) salts as starting materials because of the solubility and stability of these species in aqueous baths. Furthermore the electrochemistry of these ionic species is well understood to allow optimization of the electrodeposition of copper selenide-based compounds.

Though the chemical mechanism of the formation of $CuInSe_2$ by electrodeposition is not completely understood, it is believed by many authors that it starts with the formation of a copper selenide phase Cu_xSe_y, which can be represented by Cu_2Se. This phase is probably obtained by spontaneous reaction between deposited Cu and Se or either by reaction of deposited Cu with Se^{4+} species in solution or by reaction of deposited Se with the solution Cu^{2+} ions.

Electroreduction of this Cu_2Se phase leads to Cu which reacts with deposited Se to give further Cu_2Se and dissolved Se^{2-} which at pH ~2.5 – 3, is likely H_2Se. This latter phase reacts with In^{3+} species in solution to form In_2Se_3 at electrode surface which is then rapidly assimilated in the growing CIS layer by reaction with the Cu_2Se phase. Overall reactions can therefore be given as follows:

$$Cu_2Se(s) + 2H^+ + 2e^- \rightarrow 2Cu(s) + H_2Se(aq)$$

$$2In^{3+} + 3H_2Se(aq) \rightarrow In_2Se_3(s) + 6H^+$$

$$In_2Se_3(s) + Cu_2Se(s) \rightarrow 2CuInSe_2(s)$$

3.1 Composition and morphology

At a constant and well defined deposition potential, composition and morphology of electrodeposited CIS samples depend upon solution concentrations of Cu^{2+}, Se^{4+} and In^{3+} ionic species.

At a given deposition potential, careful control of these chemical parameters is therefore one of the key points to obtain high quality and reproducible CIS layers.

The influence of initial bath concentrations has been carried out by varying the solution concentration of one electro-active ionic element while maintaining constant concentrations of the two other species.

Figure 1 shows the compositions of electrodeposited CIS films as function of the selenium molar concentration in the bath; copper and indium solution concentrations being respectively fixed to 2.00 mM and 3.89 mM. At low Se bath concentrations, copper rich deposits are obtained which resulted in porous and powdery materials showing particles of different sizes as highlighted in insert (**a**) of Figure 1, which corresponds to a selenium molar concentration of 2.30 mM.

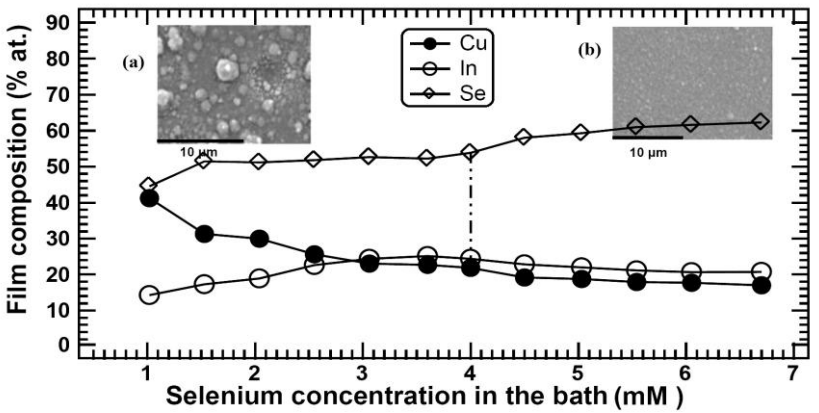

Fig. 1: Variation of CIS film composition with SeO_2 concentration in the plating bath: $[Cu^{2+}]$ = 2.00 mM and $[In^{3+}]$ = 3.89 mM

With increasing $[Se^{4+}]$ in the bath up to 3.00 mM, indium and selenium contents in the electrodeposited films slightly increase while the level of deposited copper decreases. This improves film adhesion and decreases the number of particles as well as their sizes, leading to denser, smoother and more uniform silvery-gray layers as shown in Figure 2, which corresponds to $[Se^{4+}]$ of 4.00 mM.

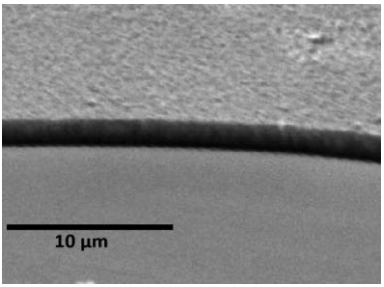

Fig. 2: SEM micrograph of a CIS film deposited using the following bath composition: $[Cu^{2+}]$ = 2.00 mM, $[Se^{4+}]$ = 4.00 mM and **[**In^{3+}] = 3.89 mM

The composition of this film was found to be Cu: 23.05 at %, In: 25.08 at % and Se: 51.87 at % and it's cross-section shows a compact structure highlighting a columnar grain growth. The material observed in the foreground of this image is the Mo surface electrode.

For $[Se^{4+}]$ greater or equal to 4.50 mM, little changes are observed in the level of deposited Cu, In and Se in the films but the layers appear less smooth, dark-gray and are composed of small particles of more uniform size as shown in insert (**b**) of Figure 1. In this compositional study, lithium and potassium species present in the electrolytic bath have not been detected in the EDS results of the electrodeposited CIS layers.

Figure 3 illustrates the variations atomic composition of CIS films with $[In^{3+}]$ in the chemical bath. For $[Cu^{2+}]$ and $[Se^{4+}]$ of 2.00 mM and 4.00 mM, respectively little change is observed in the copper content of the electrodeposited CIS films as $[In^{3+}]$ in the plating bath varies.

One can note that once $[In^{3+}]$ reaches 3.89 mM, these films become slightly copper poor and their compositions which are close to the stoichiometry, remain almost constant. At low $[In^{3+}]$ in solution these layers are characterized by the growth of small particles together with a number of larger particles imbedded in the film surface (insert (**a**) of Fig. 3).

These particles may be due to the presence of amorphous elemental Se and/or other copper selenides. At high $[In^{3+}]$ in the plating bath, CIS films are less dense and are distinguished by features having the cauliflower-like structure (insert (**b**) of Fig. 3).

For $[In^{3+}]$ in the plating bath at around 3.89 mM dense, smooth and near stoichiometric films similar to film shown in the SEM image of Figure 2 are obtained.

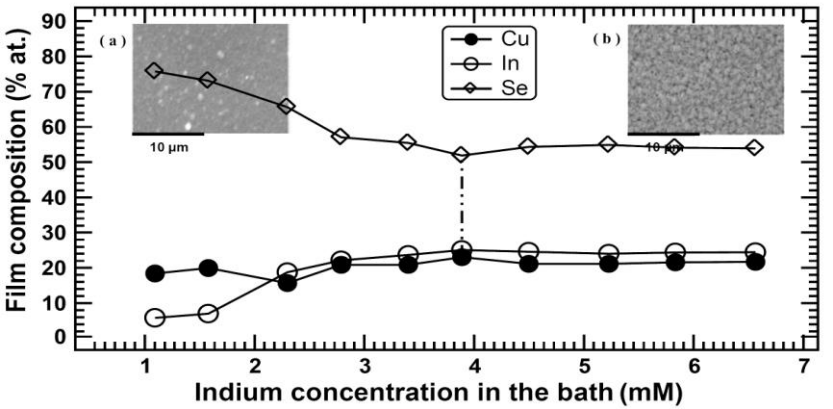

Fig. 3: Variation of CIS film composition with In^{3+} concentration in the plating bath: $[Cu^{2+}]$ = 2.00 mM and $[Se^{4+}]$= 4.00 mM

Figure 4 shows film composition as function $[Cu^{2+}]$ in the solution. Samples electrodeposited at low copper concentrations resulted in dark, powdery and very selenium rich films characterized by poor adhesion (insert (**a**) of Fig. 4). These film surfaces show also a cauliflower structure with an underlying layer which consists of small particles.

As $[Cu^{2+}]$ in the bath increases up to 4 mM, copper content in the film increases as well. For $[Cu^{2+}]$ equal to 2.00 mM the deposited films are near stoichiometric and show the dense and smooth structure as that shown in the SEM image of Figure 2.

At $[Cu^{2+}]$ greater or equal to 4 mM, copper level in the deposits is as high as selenium. This usually resulted in films peeling off during deposition. At these high copper concentrations in the bath, the films exhibit larger particle sizes compared to

particles observed in films deposited at low [Cu^{2+}] in the bath (insert (**b**) of Fig. 4). These larger particles are likely copper rich phases.

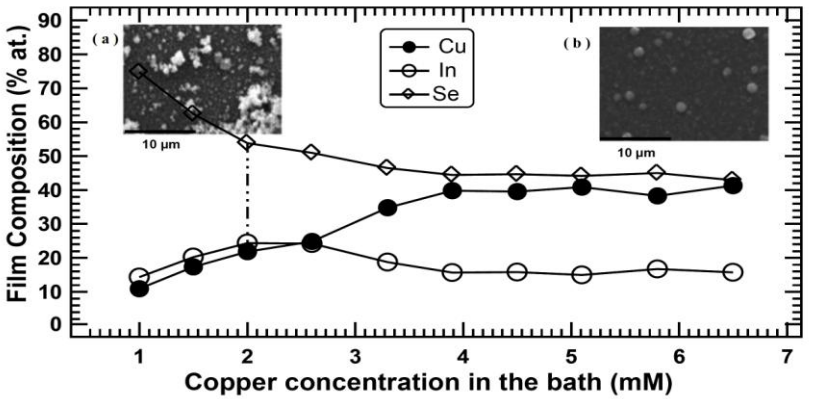

Fig. 4: Variation of CIS film composition with Cu^{2+} concentration in the plating bath: [In^{3+}] = 3.89 mM and [Se^{4+}]= 4.00 mM

A successful photovoltaic device fabrication requires careful control of composition as well as morphology of the electrodeposited CIS absorber layers. CIS films consisting of prominent large particles, cauliflower florets and others non-uniformities are undesirable.

Such defects features correspond to phases containing amorphous elemental Se or Cu-rich phases. Furthermore, large particles observed in the electrodeposited film surfaces seem to start their formation at the early stage of the growth and continues during the entire growth of the CIS layer. Such defect structures can lead to shunting effects in the photovoltaic devices.

3.2 X-ray diffraction

Energy dispersive spectroscopy (EDS) and scanning electron microscopy (SEM) investigations allowed determination of the appropriate bath composition which leads to near stoichiometric CIS films of good morphology. These optimized bath concentrations corresponding to vertical dash lines shown in Figures 1, 3 and 4 are [Cu^{2+}] = 2.00 mM, [In^{3+}] = 3.89 mM and [Se^{4+}] = 4.00 mM.

X-ray diffraction analysis was then carried out on samples grown with these bath compositions to identify the structure and phases in grown layers before and following the post-deposition treatment in H_2Se/Ar. XRD patterns measured for a sample before and following its annealing, are shown in Figure 5.

For the as-deposited CIS film (Fig. 5a-), broad and weak peaks corresponding to reflections from the (112), (204/220) and (312) planes of the chalcopyrite structure (JCPDS 40-1487) are observed. This pattern exhibits a high degree of amorphous and micro-crystalline phases with some degree of (112) preferred film orientation during film growth.

Annealing in H_2Se improves crystalline properties and better identifies the chalcopyrite crystal structure of the electrodeposited CIS films (Fig. 5b-). Furthermore, the pattern of the selenized films exhibit a pronounced (112) preferred film orientation. It is interesting to note that the (112) orientation is desirable for getting lattice match

between the CIS film and the CdS window layer in the CIS/CdS based solar cell and therefore a higher solar cell efficiency.

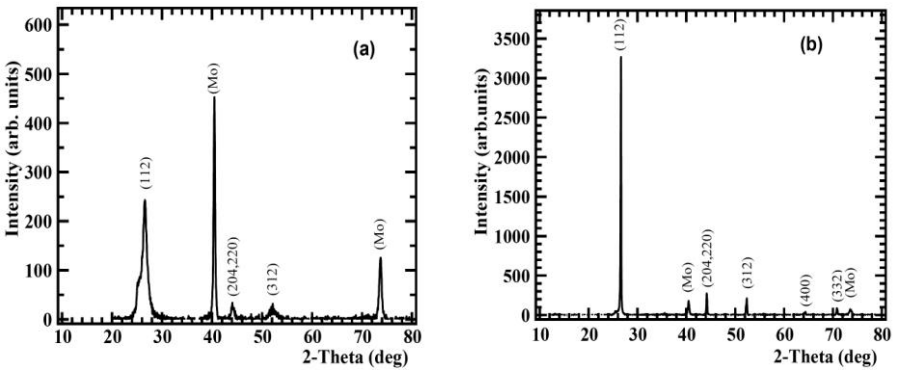

Fig. 5: XRD spectra of **(a)** as-deposited and **(b)** H_2Se-annealed CIS sample

At annealing temperatures equal or higher than 500°C, CIS samples exhibited cracking and peeling off when the selenization process is performed for duration higher than 15 minutes. For a short annealing duration, the films did not peel off from the substrate but cracking have been observed and XRD results revealed an uncompleted recrystallization process.

Post-deposition treatments performed at 450ºC for 20 minutes resulted in well-crystallized and good quality CIS layers suitable for a photovoltaic device processing. These observations are in good agreement with results reported by Guillén *et al.* [13] on recrystallization studies of CIS films electrodeposited from a sulfate-based solution. They concluded that the highest degree of recrystallization is achieved at 400ºC for CIS samples deposited at – 0.500V/SCE and that higher temperatures are required to achieve the same degree of crystallinity for samples electrodeposited at more negative potentials.

Taking into account the fact that the chalcopyrite phase of CIS has a tetragonal structure, the lattice parameters of our CIS samples have been calculated to be a = b = 5.795 Å and c = 11.590 Å in good agreement with those reported in the literature [14]. Based on the full-width at half-maximum (FWHM) of the reflection from (112) plane, the grain size of the films was estimated using the Scherrer's formula to be 783 Å.

3.3 Optical analysis

The optical transmittance and reflectance spectra were recorded for the H_2Se-selenized CIS films electrodeposited on a conductive transparent ITO substrate in order to evaluate the optical energy band-gap (E_g) and the absorption coefficient (α). In fact, the fundamental absorption in a semiconductor material can be used to determinate the energy band-gap according to the relationship:

$$(\alpha h\nu) = A^*(h\nu - E_g)^n / h\nu$$

where α is the absorption coefficient of the material, $h\nu$ the photon energy (eV), ν the light frequency, h the Planck's constant, E_g the optical band gap of the material, A^* a constant which is related to the effective masses of both electrons and holes in the

bands and n being a constant associated with the nature of the optical transition in the material (direct allowed, direct forbidden, indirect allowed or indirect forbidden transitions).

For a direct allowed transition n assumes the value 1/2 and the plot of $(\alpha h\nu)^2$ versus photon energy ($h\nu$), forms a straight line whose intercept with the $\alpha=0$ axis yields the value of the energy band gap, (E_g).

In addition, from the transmittance and reflectance values of a film, one can get its absorption coefficient α through the well-known relation:

$$\alpha = \frac{1}{d} \times \ln\left[\frac{100 - R\%}{T\%}\right]$$

$T\%$ and $R\%$ are respectively the transmittance and reflectance of the samples and 'd' the film thickness.

Figure 6 shows spectral distribution of the transmittance (T) and reflectance (R) for a CIS film grown with the optimized bath conditions and annealed in H_2Se/Ar atmosphere. Interference patterns are observed in the reflectance spectrum with a sharp fall of transmittance at the band edge which is an indication of good crystallinity of the CIS sample.

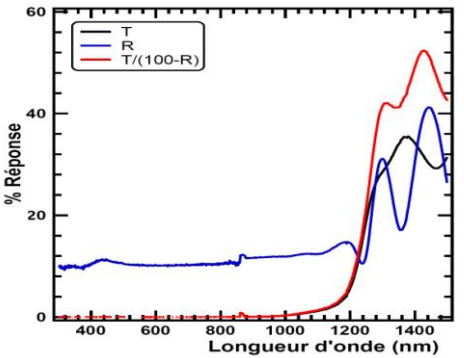

Fig. 6: Transmittance and reflectance spectra of a H_2Se-annealed CIS sample

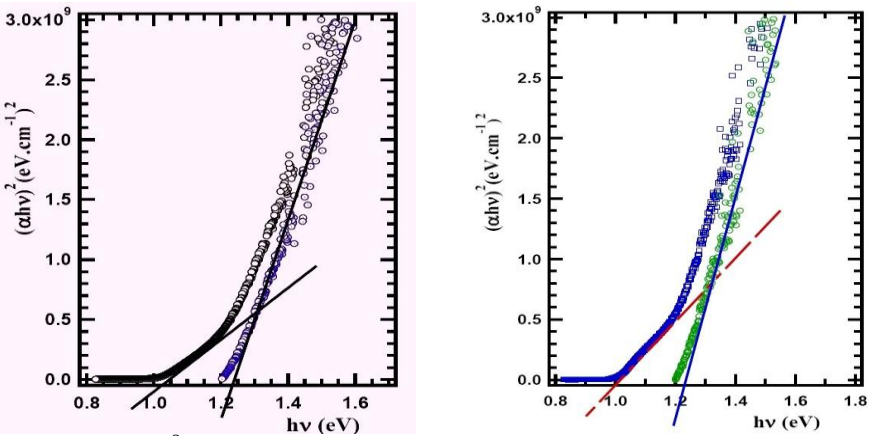

Fig. 7: $(\alpha h\nu)^2$ as a function of photon energy for a H_2Se-annealed CIS sample

The band-gap energy (E_g) and the spin-orbite parameter (Δ_{so}) of the film have been obtained from the curve shown in Figure 7.

In fact, three transitions are predicted from the electronic structure of the chalcopyrite materials due to crystal field effect and spin-orbit interaction. In the case of the $CuInSe_2$, it has been shown that crystal field is zero [14]. So, using straight line fits, (E_g) and (Δ_{so}) have been obtained from Fig. 7 to be 1.01 eV and 0.23 eV respectively. These results are also in good agreement with values reported in the literature [14]. Figure 8 shows the relationship between of the absorption coefficient (α) of the electrodeposited CIS layers and the photon energy (hν). In the visible-near infrared spectral range, figure 8 shows that the CIS layers exhibit relatively high α values (10^4~10^5) cm^{-1}.

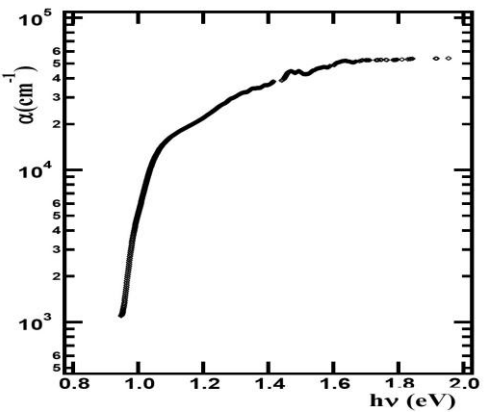

Fig. 8: Absorption coefficients as function of photon energy for an H_2Se-annealed CIS sample

3.4 Current-voltage characteristics

The performances of the Mo/CIS/CdS/ZnO-based photovoltaic devices were analyzed by recording the $J-V$ characteristics. Measurements were performed at AM 1.5 conditions (100 mW/cm^2) on 0.47 cm^2 solar cells. Figures 9 displays the current density (J) vs. voltage (V) curves of photovoltaic devices. For devices processed with CIS absorber layers deposited using the optimized bath conditions (Fig. 9-a), the open circuit voltage (V_{oc}), the short-circuit current density (J_{sc}) and the fill factor (FF) are 0.398 V, 33.30 $mA.cm^{-2}$ and 65.4 % respectively. The power efficiency of this device is 8.65%.

Changes in the electrodeposition solution concentration, even slightly far from the optimized bath conditions, cause a drop in the device efficiency. This can be observed in Fig. 9-b, where indium concentration in the bath has been raised to 4.49 mM, in Fig. 9-c where selenium concentration has been decreased to 3,6 mM and in Fig. 9-d where copper concentration in solution is 2.20 mM.

SEM analyses of the electrodeposited films demonstrated that samples grown with bath compositions which deviated from optimized conditions appeared more or less porous and their surfaces consisted of large particles, cauliflower features and others non-uniformities. In the case of Mo/CIS/CdS/ZnO substrate solar cell structure,

absorber density is critical. It can avoid diffusion of chemical species during the CBD CdS buffer and ZnO window layers deposition processes.

Less dense CIS absorber films should result in high series resistance which could lead to lower FF. Large particles observed in the electrodeposited CIS film surfaces which are Cu-rich phases lead to shunting effects in the photovoltaic devices.

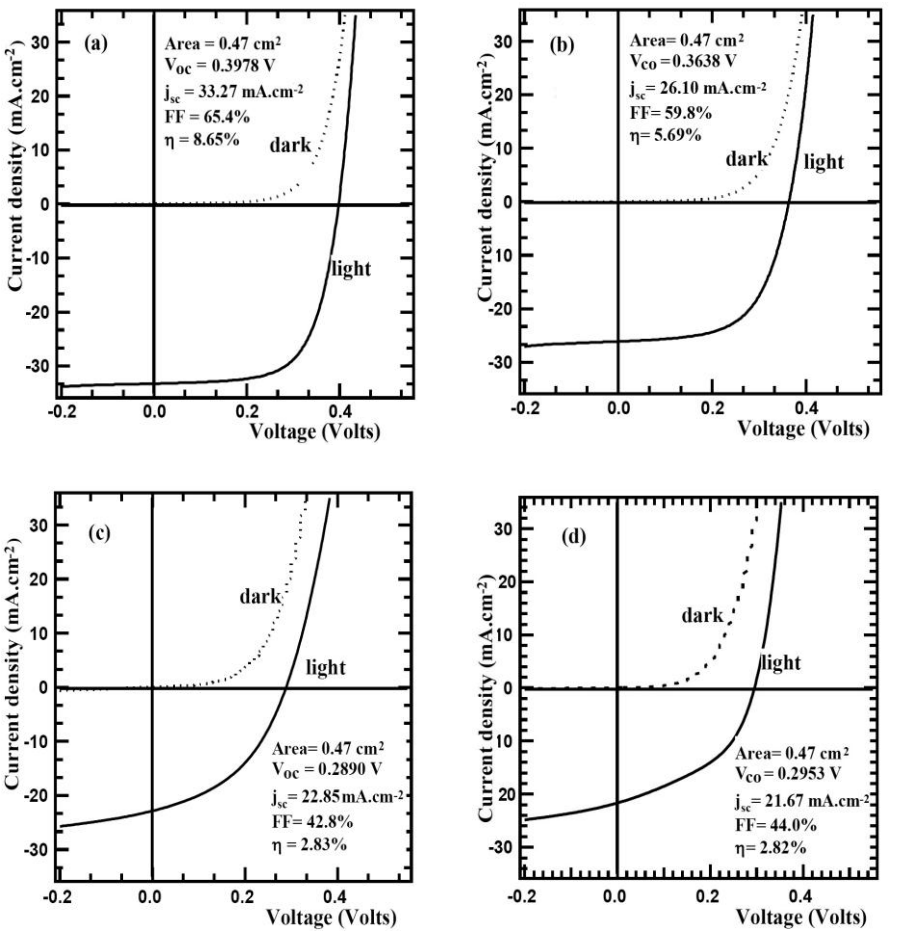

Fig. 9: Current-voltage characteristics of a CIS/CdS photovoltaic device processed with optimized deposition conditions
a) $[Cu^{2+}]$ = 2.00 mM, $[In^{3+}]$ = 3.89 mM and $[Se^{4+}]$ = 4.00 mM
b) $[Cu^{2+}]$ = 2.00 mM, $[In^{3+}]$ = 4.49 mM and $[Se^{4+}]$ = 4.00 mM
c) $[Cu^{2+}]$ = 2.00 mM, $[In^{3+}]$ = 3.89 mM and $[Se^{4+}]$ = 3.60 mM
d) $[Cu^{2+}]$ = 2.20 mM, $[In^{3+}]$ = 3.89 mM and $[Se^{4+}]$ = 4.00 mM

Table 1 summarized photovoltaic characteristics of devices corresponding to figure 9 and highlighted differences in series resistance {1.48 Ω/cm^2 for cell (a) vs. 2.12 Ω/cm^2, 4.09 Ω/cm^2 and 3.04 Ω/cm^2 for cell (b), cell (c) and cell (d), respectively} as well as in shunt conductances {1.47 mS/cm^{-2} for cell (a) vs. 3.84 mS/cm^{-2}, 21.00 mS/cm^{-2} and 25.00 mS/cm^{-2} for cell (b) and cell (c) respectively}.

Table 1: Photovoltaic characteristics of CIS/CdS-based solar cell

Cell	V_{OC} (V)	J_{SC} (mA/cm^2)	FF (%)	R_{OC} (Ω/cm^2)	G_{SC} (mS/cm^{-2})	Eff (%)
a-	0.3978	33.30	65.4	1.48	1.47	**8.65**
b-	0.3638	26.10	59.8	2.12	3.84	**5.69**
c-	0.2890	22.85	42.8	4.09	21.00	**2.83**
d-	0.2953	21.67	44.0	3.04	25.00	**2.82**

4. CONCLUSION

One step electrodeposition has been used to deposit thin $CuInSe_2$ films from low concentration sulfate-based electrolytic solution. Compositional and morphological properties of the films have been analyzed together with structural and optical properties.

This study showed that film structure and composition are closely linked and largely influenced by the initial bath composition of electro-active ionic species. Careful attention allowed selecting appropriate deposition conditions for growth of polycrystalline near stoichiometric films, free from secondary phases, showing smooth surfaces, columnar structure and pronounced (112) preferred orientation. These high quality electrodeposited $CuInSe_2$ thin layers led to ~ 9% solar cell devices.

ACKNOWLEDGEMENTS

A part of this work has been done at Institute of Energy conversion (IEC), University of Delaware and was supported by the J. William Fulbright Foreign Scholarship Board and the Bureau of Educational and Cultural affairs, United States Department of State. The authors are grateful to IEC stuff members for valuable technical discussions.

REFERENCES

[1] J.R. Tuttle, M.A. Contreras, J.J. Gillespie, K.R. Ramanathan, A.L. Tennant, J. Keane, A.M. Gabor and R. Noufi, '*Accelerated Publication 17.1 % Efficient Cu(In,Ga)Se_2-Based Thin Film Solar Cell*', Progress in Photovoltaics: Research and Applications, Vol. 3, N°4, pp. 235 - 238, 1995.

[2] A. Romeo, M. Terheggen, D. Abou-Ras, D.L. Bätzner, F.J. Haug, M. Kälin, D. Rudmann and A.N. Tiwari, '*Development of Thin-Film Cu(In,Ga)Se_2 and CdTe Solar Cells*', Progress in Photovoltaics: Research and Applications, Vol. 12, N°2-3, pp. 93 – 111, 2004.

[3] M. Contreras, K. Ramanathan, J. Abushama, F. Hasoon, D.Young, B. Egaas and R. Noufi, '*Diode Characteristics in State-of-the-Art ZnO/CdS/Cu($In_{1-x}Ga_x$)Se_2 Solar Cells*', Progress in Photovoltaics: Research and Applications, Vol. 13, N°3, pp. 209 – 216, 2005.

[4] D. Cunningham, M. Rubcich and D. Skinner, '*Cadmium Telluride PV Module Manufacturing at BP Solar*', Progress in Photovoltaics: Research and Applications, Vol. 10, N°2, pp. 159 – 168, 2002

[5] R.N. Bhattacharya, W. Batchelor, K. Ramanathan, M.A. Contreras and T. Moriarty, '*The Performance of $CuIn_{1-x}Ga_xSe_2$-Based Photovoltaic Cells Prepared from Low-Cost Precursor Films*', Solar Energy Materials and Solar Cells, Vol. 63, N°4, pp. 367 – 374, 2000.

[6] D. Lincot, J.F. Guillemoles, S. Taunier, D. Guimard, J. Sicx-Kurdi, A. Chaumont, O. Roussel, O. Ramdani, C. Hubert, J.P. Fauvarque, N. Bodereau, L. Parissi, P. Panheleux, N. Fanouillere, N. Naghavi, P.P. Grand, M. Benfarah, P. Mogensen and O. Kerrec, '*Chalcopyrite thin Film Solar Cells by Electrodeposition*', Solar Energy, Vol. 77, N°6, pp. 725 –737, 2004.

[7] R.N. Bhattacharya, W. Batchelor, J.F. Hiltner and J.R. Sites, '*Thin Film $CuIn_{1-x}Ga_xSe_2$ Photovoltaic Cells from Solution-Based Precursor Layers*', Applied Physics Letters, Vol. 75, N°10, pp. 1431 – 1433, 1999.

[8] J.F. Guillemoles, P. Cowache, A. Lusson, K. Fezzaa, F. Boisivon, J. Vedel and D. Lincot, '*One Step Electrodeposition of $CuInSe_2$: Improved Structural, Electronic and Photovoltaic Properties by Annealing under High Selenium Pressure*', Journal of Applied Physics, Vol. 79, N°9, pp. 7293 – 7301, (1996).

[9] J.R. Tuttle, T.A. Berens, S.E. Asher, M.A. Contreras, K.R. Ramanathan, A.L. Tennant, R. Bhattacharya, J. Keane and R. Noufi, Proceedings of the 13th European Photovoltaic Solar Energy Conference, Nice, pp. 2131 - 2131-2134, 1995.

[10] S.N. Qiu, L. Li, C.X. Qiu, I. Shih and C.H. Champness, '*Study of $CuInSe_2$ Thin Film Prepared by Electrodeposition*', Solar Energy Materials and Solar Cells, Vol. 37, N°3-4, pp. 389 – 393, 1995.

[11] M. Engelmann, B.E. McCandless and R.W. Birkmire, '*Formation and Analysis of Graded $CuIn(Se_{1-y}S_y)_2$ Films*', Thin Solid Films, Vol. 387, N°1-2, pp. 14 – 17, 2001.

[12] W.N. Shafarman, R. Klenk and B.E. McCandless, '*Device and Material Characterization of $Cu(InGa)Se_2$ Solar Cells with Increasing Band Gap*', Journal of Applied Physics, Vol.79, N°9, pp. 7324 – 7328, 1996.

[13] C. Guillen and J. Herrero, '*Recrystallization and Components Redistribution Processes in Electrodeposited $CuInSe_2$ Thin Film*', Thin Solid Films, Vol. 387, N°1-2, pp. 57 – 59, 2001.

[14] J.L. Shay and J.H. Wernick, '*Ternary Chalcopyrite Semiconductors: Growth, Electronic Properties, and Applications*', Oxford, New York, Pergamon Press, 244 p., 1975.